Crystalline Accommodation Law Modeling for the Structure of Inorganic Perovskite Halides Used in Solar Cells

Ansam Gaber [1,*], Zeinab Mohammed[1], Eman Elesh[1], Tarek El Ashram[1]

[1]Physics Department, College of Science, Port Said University, Port Said, Egypt

*Corresponding author: **ansamgaber@sci.psu.edu.eg**

_____

ABSTRACT

Perovskite halides are very important materials used in solar cell manufacturing. The efficiencies of perovskite solar cell have increased from 3.8 % to more than 25 % within the last 11 years. Several models were developed to predict the perovskites formability such as; Goldschmidt tolerance factor (t), Rohere octahedral factor (μ), t-μ 2D structure map and finally the new tolerance factor (τ). All the previous models are empirical and geometrical and have no theoretical basis. In addition these models cannot predict the formation of perovskite structure. Crystalline accommodation law (CAL) by Tarek El Ashram could explain successfully the crystal structure of crystalline materials in terms of their valence electron concentrations (VEC). Therefore the aim of this work is to use CAL for modeling perovskite halide structures. Here we show that CAL is succeeded in prediction of the perovskite halide structures as the following; all the perovskite halides are formed at VEC = 4.8 and most of them crystallize in three systems; cubic, hexagonal and orthorhombic with the number of filled zones in the valence band $(\frac{V_F}{V_B}) =$ 12, 24 and 48 respectively. We also found the most suitable IPH compounds for solar cells applications are orthorohmbic compounds that have minimum E_F, minimum V_B and the maximum number of filled zones in the valence band.

Key Words:

Perovskite halides, Volume of quantum state, Solar Cell, Crystalline accommodation law.
_____

1. INTRODUCTION

Inorganic perovskite halides (IPH) have gained great success in manufacturing solar cell panels that can be determined to be the most important sources of renewable energy. It can convert the solar radiation of sunlight directly into electrical renewable current and can reach sunlight without any efforts. One of the most important of IPH uses are costless comparable to Si in solar cell panels, stable, outstand of photovoltaic phenomena, used in the design of optoelectronic devices etc [1- 5].

In the last decade, efficiency of perovskite solar cells jumped from 3.8% to more than 25 % in a very short span of time achieving an incredible increase in efficiency due to the easiest way of using perovskites as tandem [6-13]. There are two characters distinguished any IPH the first is chemical formula ABX_3 where A and B are different sizes monovalent and divalent cations respectively and X is a

halogen anion (F−,Cl−, Br−, I−) and the second is an octahedron shape inside the crystal produced by B and X atoms as shown in Fig. 1.
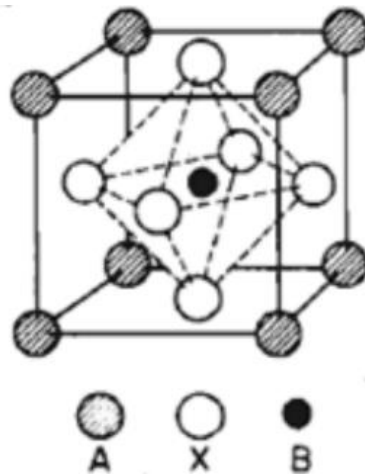

Fig. 1: Crystal structure of perovskite halides [14].

Different attempts tried to explain the formability of IPH compounds based on the size ratio and the geometry of the distribution of the ions. The first attempt was in 1927 by Goldschmidt who supposed the tolerance factor t from the ionic radius concepts given by;

$$t = \frac{r_A + r_X}{\sqrt{2}(r_B + r_X)} \qquad (1)$$

where r_A, r_B and r_X are ionic radius of A, B cations and X halogen anion (F−, Cl−, Br−,I−) respectively. If t has values 0.9: 1 then the structure predicted is cubic, if t is higher than one, then the structure predicted is hexagonal or tetragonal and if the value of t is in between 0.71: 0.9 then the predicted structure is orthorhombic or rhombohedral structure [15].

In 2001, Rohere [16] proposed an octahedral factor μ given by;

$$\mu = {r_B}/{r_X} \qquad (2)$$

where r_B and r_X are ionic radius of B cation and X halogen anion respectively. By the same way of the last model, the stability of perovskite halides structure achieved when the value of μ is in between 0.377 and 0.895. After 7 years, Li et al [17] designed a model called t-μ 2D structure map model that basically depended on the last two models of Goldschmidt and Rohere as the scientists found that the value of t or μ only not sufficient in order to define perovskites compounds. They did studies on 186 IPH compounds using structure map and they found that only 7 compounds of total 186 IPH not follow structural map and not determined to be IPH. After that in 2019, Christopher J. Bartel et al [18] modified t to new tolerance factor τ to predict the formation of perovskites. The new tolerance factor τ is given by;

$$\tau = \frac{r_X}{r_B} - n_A \left(n_A - \frac{{r_A}/{r_B}}{\ln({r_A}/{r_B})} \right) \qquad (3)$$

where r_A and r_B are ionic radius of A and B cations and r_X is the ionic radius of the anion respectively, and n_A is the oxidation state of A atom. This study doing on thousands of perovskites types including halides which increase the correction of the possibilities of perovskite compound production to 92%, 90%, 93% and 91% for fluorides, chlorides, bromides and iodides respectively than in case of Goldschmidt tolerance factor. All the previous models are empirical and geometrical and have no theoretical basis. In addition these models cannot predict the formation of perovskite structure, and cannot determine the electronic structure of perovskite compounds.

Hume Rothery valence electron concentration (VEC) rule [19] had taken the valence electron interaction into account and succeeded in prediction of the structure of some types of compounds and failed to extend to the other types of compounds. Based on this idea in 2017, Tarek El Ashram

[20] succeeded in explanation the crystalline structure of materials such as pure metals and different types of compounds by using the crystalline accommodation law (CAL). CAL relates both the volume of Fermi sphere V_F and the volume of Brillouin zone V_B by *VEC* and is given by;

$$\frac{V_F}{V_B} = \frac{n\,VEC}{2} \qquad (4)$$

CAL gives the number of filled zones in the valence band and can be applied to any crystalline materials. Therefore, we aimed in this study to use CAL for modeling the crystalline structure of IPH compounds in terms of their VEC.

2. COMPUTATIONAL METHODOLOGY

The computational methodology was based on CAL. The parameters in CAL are *VEC, n, V_F* and *V_B*. These parameters were calculated from the crystal structure data obtained from JCPDS cards [21] shown in Table 1 as the following;

1- *VEC is defined in [19] and in this case is given by;*

$$VEC = \frac{VEC\ of\ A + VEC\ of\ B + VEC\ of\ X}{5} \qquad (5)$$

The IPH molecule consists of 5 atoms, 2 cations A and B and 3 anions X. According to the charge neutrality of the molecule, the charge on cations must equal to the charge on the anions. Therefore, the charge on A is always +1 and the charge on B is always +2 which equal the charge -3 on the anions X. Thus, the atom A will contribute one electron and the atom B will contribute two electrons, which are shared with seven electrons of the halogen atom X. Consequently, let us take some examples;

For $CsHgBr_3$ VEC$=\frac{1*1+1*2+3*7}{5}=4.8$, $CsCuBr_3$ VEC $=\frac{1*1+1*2+3*7}{5}=4.8$ and for $CsCrBr_3$ VEC $=$

$$\frac{1*1+1*2+3*7}{5}=4.8.$$

Actually it was found that all IPH compounds are formed at VEC = 4.8.

2- The number of atoms per lattice point *n* is the number of atoms in the primitive cell was obtained from diffraction data shown on Table 1.

3- V_F was calculated by;

$$V_F = \frac{4}{3}\pi K_F^3 \qquad (6)$$

where K_F is given by;

$$K_F^3 = \frac{3\pi^2(0.6022)n\,VEC\,Dx}{Mwt} \qquad (7)$$

where *Dx* is the density from X-ray diffraction data and *Mwt* is the molecular weight

4- V_B is) given by;

$$V_B = \frac{8\pi^3}{V_P} \qquad (8)$$

where V_P was obtained from the lattice parameters.

The calculations were carried out on the IPH compounds, which are stable at room temperature shown in Table 1.

3. RESULTS AND DISCUSSION

The calculated parameters of CAL for IPH compounds are shown in Table 2. It is evident that all of IPH compounds are formed at the same VEC = 4.8 and corresponding to the charge nutrality of the molecule. It was found that IPH compounds crystalize in three main systems, cubic, hexagonal and orthorohmbic. For the cubic system it was found that n equal to 5, this means that every primitive cell

contains only one molecule. It was also found that $\frac{V_F}{V_B} = 12$. For the hexagonal system it was found that n equal to 10, this means that every primitive cell contains two molecules. It was also found that $\frac{V_F}{V_B} = 24$ For the orthorohombic system it was found that n equal to 20, this means that every primitive cell contains four molecules. It was also found that $\frac{V_F}{V_B} = 48$.

Fig. 2a. shows the variation of Bz volume with the primitive cell volume V_P. It shows that V_B decreases by increasing V_P as predicted by equation (8), this means that as V_P increases the volume of quantum state decreases, since Bz contains only one quantum state.
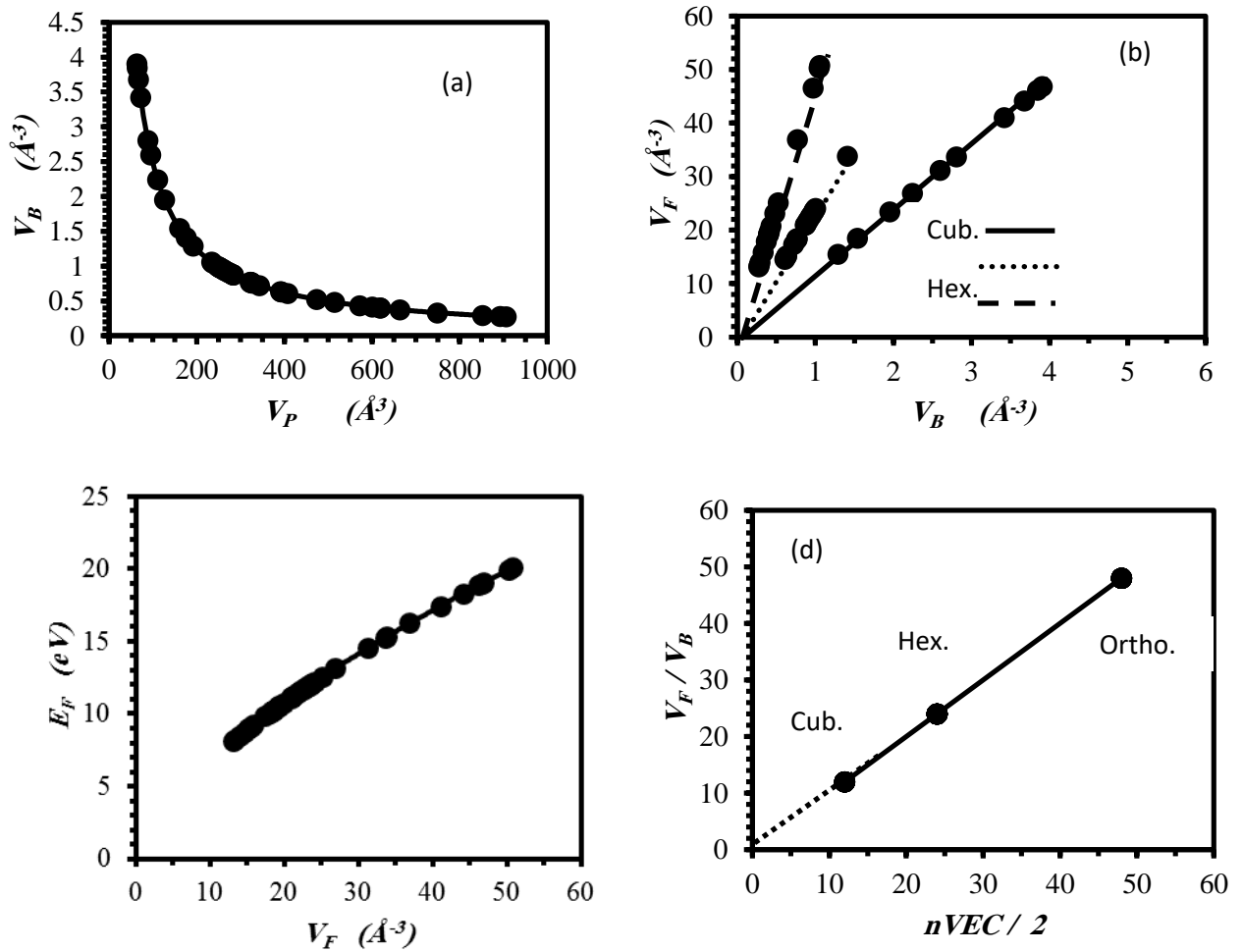

Fig. 2: (a) the variation of Bz volume with the primitive cell volume. (b) the variation of Fermi sphere volume with Bz volume. (c) the variation of Fermi energy with Fermi sphere volume. (d) verification of CAL for IPH compunds.

The volume of primitive cell increases by incrasing the number of molecules in the primitive cell. The maximum V_P was found for orthorohombic system which has 4 molecules (20 atoms) in the primitive cell. The minimum V_P was found for cubic system which has only one molecules (5 atoms) in the primitive cell. The maximum volume of quantum state V_B was found for cubic system (since it has the minimum V_P) and the minimum was found for orthorohmbic system (since it has the maximum V_P). Fig. 2b. shows the variation of Fermi sphere volume with Bz volume. It shows that V_F increases linearly with V_B according to CAL for the three crystalline systems (cubic, hexagonal and orthorohmbic). The maximum volume of Fermi sphere was found for orthorohmbic system $V_F = 50.81$ Å^{-3} for $NaZnF_3$. And

the minimum was found for also orthorohmbic system $V_F = 13.14$ $\mathring{A}^{-3}$ for $CsCaI_3$. Fig. 2c shows the variation of Fermi energy with Fermi sphere volume. It shows that E_F increases by increasing V_F up to maximum value 20.11 eV for $NaZnF_3$ orthorohombic compound. The minimum value of E_F was found to be 8.16 eV for $CsCaI_3$ orthorohmbic compound. On the average E_F is greater for orthorohmbic system than cubic system and is small for hexagonal system. Fig. 2d shows the relation between V_F/V_B and nVEC/2. It shows that a linear relation as predicted by CAL. That means verification of CAL for IPH compounds. The valence band structure found from CAL for cubic IPH compounds is 12Bz, for hexagonal IPH compounds is 24Bz and for orthorohmbic IPH compounds is 48Bz. The orthorohmbic $CsPbI_3$ compound has large applications in solar cells manufacturing [21-24]. The electronic properties of $CsPbI_3$ (in the present work) was found to be valence band structure, 48Bz, $E_F = 8.24$ eV and $V_B = 0.277$ $\mathring{A}^{-3}$. From the results found for $CsPbI_3$ orthorhombic compound, it is evident that the most suitable IPH compunds for optoelectronic applications are orthorohmbic compounds that have minmum E_F, minimum V_B and the maximum number of filled zones in the valence band. In this orthorohmbic group the candidate to replace $CsPbI_3$ compound, because of the toxicity of Pb, are two compounds that give the same electronic structure of $CsPbI_3$. The first compound is $CsCaI_3$, with valence band structure 48Bz, $E_F = 8.16$ eV which is the minimum value of all compounds and $V_B = 0.273$ $\mathring{A}^{-3}$, which is also the minimum value of all compounds. The second compound is $KGeI_3$ with valence band structure 48Bz, $E_F = 9.26$ eV and $V_B = 0.331$ $\mathring{A}^{-3}$.

Some tetragonal forms were found for perovskite halide compounds and are shown in Table 3. It is clear from Table 3 that the lattice parameters *a* and *c* of these compounds are very close so that they may be considered as distorted cubic. By applying CAL on these compounds we obtained the results shown in Table 4. From Table 4 it is clear that these compounds are formed at the same VEC= 4.8 and at the same $V_F/V_B = 12$ as for cubic compounds. This result confirm the cubic structure of these compounds.

4.   CONCLUSION

In conclusion, CAL succeeded in explanation and prediction of the structures of IPH compounds in terms of their valence electron concentration VEC, volume of Fermi sphere V_F and volume of Brillouin zone V_B. It also determines their electronic structures of the valence band, which were found to be; for cubic IPH compounds 12Bz, for hexagonal IPH compounds 24Bz and for orthorohmbic IPH compounds 48Bz. The most suitable IPH compounds for solar cells and optoelectronic applications are orthorohmbic compounds that have minmum E_F, minimum V_B and the maximum number of filled zones in the valence band. Based on this result, two compounds can be candidates to replace $CsPbI_3$, because of the toxicity of Pb, are $CsCaI_3$ and $KGeI_3$ because they have the same electronic properties as $CsPbI_3$ without toxic elements.

Table 1 : Crystal structure data obtained from JCPDS cards for IPH compounds used in this study.

compound	System	card no.	S.G	Z	VEC	n	Dx (gm/cm^3)	Mwt (gm/mol)	a (Å)	b (Å)	c (Å)	V_P $(Å^3)$
$CsHgBr_3$	cubic	731946	Pm3m	1	4.8	5	4.955	573.21	5.77			192.1
$CsHgCl_3$	cubic	731949	Pm3m	1	4.8	5	4.537	439.85	5.44			160.989
$RbCaF_3$	cubic	840440	Pm$\bar{3}$m	1	4.8	5	3.431	182.54	4.454			88.359
$RbVF_3$	cubic	772291	Pm$\bar{3}$m	1	4.8	5	4.429	193.4	4.17			72.5117
$CsHgF_3$	cubic	771570	Pm$\bar{3}$m	1	4.8	5	6.794	390.49	4.57			95.444
$KCoF_3$	cubic	894108	Pm$\bar{3}$m	1	4.8	5	3.818	155.03	4.07			67.4191
$KNiF_3$	cubic	894109	Pm$\bar{3}$m	1	4.8	5	3.986	154.79	4.01			64.4812
$TlMnCl_3$	cubic	241301	Pm$\bar{3}$m	1	4.8	5	4.785	365.67	5.025			126.884
$KMgF_3$	cubic	862480	Pm$\bar{3}$m	1	4.8	5	3.149	120.4	3.989			63.483
$CsPbF_3$	cubic	751273	Pm$\bar{3}$m	1	4.8	5	5.962	397.1	4.8			110.592
$CsCuBr_3$	ortho	711461	C2221	8	4.8	20	4.676	436.16	12.78	7.666	12.65	619.623
$CsPbI_3$	ortho	741970	Pmnb	4	4.8	20	5.363	720.82	4.797	10.46	17.79	892.712
$KCdCl_3$	ortho	751783	Pnma	4	4.8	20	3.329	257.87	8.792	4.009	14.6	514.502
$RbCdBr_3$	ortho	700300	Pnma	4	4.8	20	4.697	437.59	9.436	4.202	15.61	618.819
$RbPbI_3$	ortho	701969	Pnma	4	4.8	20	5.248	673.38	10.27	17.38	4.773	852.326
$KGeI_3$	ortho	381226	Pnma	4	4.8	20	4.365	492.4	10.13	4.499	16.44	749.314
$RbCaCl_3$	ortho	200016	Pnma	4	4.8	20	2.564	231.91	7.541	10.67	7.469	600.805
$KCaCl_3$	ortho	211170	Pnma	4	4.8	20	2.156	185.54	7.551	10.44	7.251	571.724
$RbSrCl_3$	ortho	211426	Pnma	4	4.8	20	2.797	279.45	7.924	10.97	7.631	663.516
$KCdF_3$	ortho	840488	Pbnm	4	4.8	20	4.294	208.5	6.103	6.103	8.66	322.556
$KFeCl_3$	ortho	711415	Pnma	4	4.8	20	2.821	201.3	8.712	3.845	14.15	473.992
$NaCoF_3$	ortho	810955	Pbnm	4	4.8	20	3.899	138.92	5.422	5.606	7.786	236.661
$NaMnF_3$	ortho	790810	Pnma	4	4.8	20	3.507	134.92	5.751	8.008	5.548	255.508
$NaZnF_3$	ortho	810954	Pbnm	4	4.8	20	4.121	145.36	5.409	5.579	7.765	234.323
$CsCaI_3$	ortho	441374	Pbnm	4	4.8	20	4.059	553.7	8.555	8.623	12.28	905.999
$CsCrBr_3$	Hexa	701350	P63mc	2	4.8	10	4.347	424.61	7.588		6.506	324.404
$CsScBr_3$	Hexa	420979	P63/mmc	2	4.8	10	4.276	417.57	7.68		6.35	324.316
$CsCrCl_3$	Hexa	761708	P63/mmc	2	4.8	10	3.413	291.26	7.249		6.228	283.415
$CsCdBr_3$	Hexa	896033	P63/mmc	2	4.8	10	4.697	485.03	7.675		6.722	342.904
$RbTiCl_3$	Hexa	771690	P63/mmc	2	4.8	10	3.025	239.73	7.117		6	263.191
$RbVCl_3$	Hexa	840913	P63/mmc	2	4.8	10	3.215	242.77	6.988		5.93	250.772
$RbCoCl_3$	Hexa	741690	P63/mmc	2	4.8	10	3.274	250.76	6.999		5.996	254.362
$RbNiBr_3$	Hexa	712218	P63/mmc	2	4.8	10	4.489	383.88	7.268		6.208	283.988
$CsMgI_3$	Hexa	896034	P63/mmc	2	4.8	10	4.382	537.92	8.198		7.004	407.643
$CsMgCl_3$	Hexa	890290	P63/mmc	2	4.8	10	3.103	263.57	7.26		6.18	282.085
$CsTiBr_3$	Hexa	842420	P63/mmc	2	4.8	10	4.328	420.52	7.656		6.357	322.681
$CsTiCl_3$	Hexa	771691	P63/mmc	2	4.8	10	3.412	287.16	7.302		6.053	279.479
$CsMnI_3$	Hexa	720571	P63/mmc	2	4.8	10	4.823	568.56	8.111		6.871	391.459
$CsMnBr_3$	Hexa	701449	P63/mmc	2	4.8	10	4.343	427.56	7.609		6.52	326.904
$CsCoCl_3$	Hexa	741665	P63/mmc	2	4.8	10	3.655	298.2	7.202		6.032	270.918
$CsNiCl_3$	Hexa	870537	P63/mmc	2	4.8	10	3.738	297.96	7.171		5.944	264.701
$RbFeCl_3$	Hexa	191099	P63/mmc	2	4.8	10	3.165	247.67	7.06		6.02	259.851
$CsFeCl_3$	Hexa	180331	P63/mmc	2	4.8	10	3.575	295.11	7.237		6.045	274.177
$RbNiCl_3$	Hexa	712217	P63/mmc	2	4.8	10	3.363	250.53	6.955		5.906	247.403
$CsCrI_3$	Hexa	740870	P63/mmc	2	4.8	10	4.771	565.61	8.107		6.917	393.691
$CsNiF_3$	Hexa	780397	P63/mmc	2	4.8	10	4.692	248.6	6.236		5.225	175.961
$TlFeCl_3$	Hexa	260803	P63/mmc	2	4.8	10	4.828	366.58	6.965		6.002	252.148

Table 2: Results of CAL parameters for IPH compounds.

Compound	System	V_B (Å^{-3})	E_F(eV)	V_F (Å^{-3})	nVEC/2	V_F/V_B
CsHgBr$_3$	cubic	1.29126	9.112976	15.495	12	11.99995
CsHgCl$_3$	cubic	1.54079	10.25218	18.48953	12	12.00005
RbCaF$_3$	cubic	2.8073	15.29497	33.6918	12	12.00149
RbVF$_3$	cubic	3.42083	17.44776	41.04978	12	11.99995
CsHgF$_3$	cubic	2.59891	14.52727	31.18726	12	12.00014
KCoF$_3$	cubic	3.67923	18.31416	44.14503	12	11.99846
KNiF$_3$	cubic	3.84686	18.86702	46.15896	12	11.99912
TlMnCl$_3$	cubic	1.95493	12.0144	23.45601	12	11.99839
KMgF$_3$	cubic	3.90735	19.06358	46.88218	12	11.99846
CsPbF$_3$	cubic	2.24293	13.16745	26.91248	12	11.9988
CsCdBr$_3$	cubic	1.63817	10.67943	19.65726	12	11.99955
CsCuBr$_3$	ortho	0.40032	10.51944	19.21721	48	48.00405
CsPbI$_3$	ortho	0.27786	8.245702	13.33652	48	47.99705
KCdCl$_3$	ortho	0.48212	11.90645	23.1406	48	47.99791
RbCdBr$_3$	ortho	0.40084	10.52792	19.24043	48	47.99971
RbPbI$_3$	ortho	0.29103	8.504773	13.96996	48	48.00222
KGeI$_3$	ortho	0.33104	9.267255	15.89014	48	48.00117
RbCaCl$_3$	ortho	0.41286	10.73757	19.81801	48	48.00144
KCaCl$_3$	ortho	0.43386	11.09978	20.82921	48	48.00862
RbSrCl$_3$	ortho	0.37384	10.04845	17.94114	48	47.9912
KCdF$_3$	ortho	0.76902	16.2559	36.91625	48	48.00457
KFeCl$_3$	ortho	0.52332	12.57612	25.12007	48	48.00119
NaCoF$_3$	ortho	1.04812	19.98171	50.30951	48	47.99958
NaMnF$_3$	ortho	0.97081	18.98512	46.59304	48	47.99382
NaZnF$_3$	ortho	1.05858	20.11618	50.8182	48	48.00589
CsCaI$_3$	ortho	0.27379	8.164633	13.14033	48	47.99482
CsCrBr$_3$	Hexa	0.76463	10.20093	18.35105	24	23.99982
CsScBr$_3$	Hexa	0.76484	10.20264	18.35566	24	23.99932
CsCrCl$_3$	Hexa	0.87522	11.16205	21.00473	24	23.99939
CsCdBr$_3$	Hexa	0.72338	9.82973	17.35855	24	23.99646
RbTiCl$_3$	Hexa	0.94247	11.7267	22.61854	24	23.99914
RbVCl$_3$	Hexa	0.98915	12.11056	23.73819	24	23.99862
RbCoCl$_3$	Hexa	0.97519	11.99648	23.40356	24	23.99904
RbNiBr$_3$	Hexa	0.87345	11.14662	20.96118	24	23.99803
CsMgI$_3$	Hexa	0.6085	8.759448	14.60213	24	23.99698
CsMgCl$_3$	Hexa	0.87935	11.19689	21.10316	24	23.99868
CsTiBr$_3$	Hexa	0.76872	10.23703	18.44855	24	23.99919
CsTiCl$_3$	Hexa	0.88755	11.26584	21.29839	24	23.99692
CsMnI$_3$	Hexa	0.63366	8.999139	15.20556	24	23.99659
CsMnBr$_3$	Hexa	0.75879	10.14773	18.20767	24	23.99581
CsCoCl$_3$	Hexa	0.91559	11.50165	21.97057	24	23.99602
CsNiCl$_3$	Hexa	0.93709	11.68139	22.48759	24	23.99714
RbFeCl$_3$	Hexa	0.95459	11.82607	22.90667	24	23.9964
CsFeCl$_3$	Hexa	0.90471	11.41217	21.71469	24	24.00189
RbNiCl$_3$	Hexa	1.00261	12.22039	24.06183	24	23.99909
CsCrI$_3$	Hexa	0.63006	8.965376	15.12007	24	23.99774
CsNiF$_3$	Hexa	1.40969	15.33716	33.83128	24	23.99912
TlFeCl$_3$	Hexa	0.98375	12.06626	23.60805	24	23.99809

Table 3 : Crystal structure data obtained from JCPDS cards for IPH tetragonal compounds.

compound	System	card no.	S.G	Z	VEC	n	Dx (gm/cm³)	Mwt (gm/mol)	a (Å)	c (Å)	$V_P(Å^3)$
CsCrCl3	Tetra	200289	P4mm	1	4.8	5	3.083	326.88	5.593	5.628	176.053
CsEuCl3	Tetra	840484	P4mm	1	4.8	5	3.703	391.22	5.588	5.619	175.457
CsPbCl3	Tetra	180366	P4mm	1	4.8	5	4.228	446.46	5.584	5.623	175.331
KCrF3	Tetra	741768	P4/mmm	1	4.8	5	3.363	148.09	4.27	4.01	73.1139

Table 4: Results of CAL parameters for IPH tetragonal compounds.

Compound	System	$V_B (Å^{-3})$	$E_F(eV)$	$V_F (Å^{-3})$	nVEC/2	V_F/V_B
CsCrCl3	Tetra	1.408951	9.65822	16.9062	12	11.99916
CsEuCl3	Tetra	1.413734	9.68119	16.9666	12	12.0013
CsPbCl3	Tetra	1.414753	9.684457	16.9752	12	11.99868
KCrF3	Tetra	3.392653	17.35033	40.7064	12	11.9984

5. REFERENCES

[1] M. Ahmad, G. Rehman, L. Ali, M. Shafiq, R. Iqbal, R. Ahmad, T. Khan, S. Jalali-Asadabadi, M. Maqbool and I. Ahmad, "Structural, electronic and optical properties of CsPbX₃ (X=Cl, Br, I) for energy storage and hybrid solar cell applications," Journal of Alloys and Compounds, vol. 705, no. 25, May. 2017, doi: 10.1016/j.jallcom.2017.02.147.

[2] T. R. Cook, D. K. Dogutan, S. Y. Reece, Y. Surendranath, T. S. Teets and D. G. Nocera, "Solar Energy Supply and Storage for the Legacy and Nonlegacy Worlds," Chemical Reviews, vol. 110, no. 11, Aug. 2010, doi:10.1021/cr100246c.

[3] A. Hagfeldt, G. Boschloo, L. Sun, L. Kloo and H. Pettersson, "Dye-sensitized solar cells," Chemical reviews, vol. 110, no. 11, Oct. 2010, doi:10.1021/cr900356p.

[4] D. Saikia, J. Bera, A. Betal and S. Sahu, "Performance evaluation of an all inorganic CsGeI₃ based perovskite solar cell by numerical simulation," Optical Materials, vol. 123, Jan. 2022, doi:10.1016/j.optmat.2021.111839.

[5] P. Tonui, S. O. Oseni, G. Sharma, Q. Yan and G. T. Mola, "Perovskites photovoltaic solar cells: An overview of current status," Renewable and Sustainable Energy Reviews, vol. 91, Aug. 2018, doi:10.1016/j.rser.2018.04.069.

[6] J. Chen and Ya Wang, "Personalized dynamic transport of magnetic nanorobots inside the brain vasculature," Nanotechnology, vol. 31, no. 49, Dec. 2020, doi:10.1088/1361-6528/abb392.

[7] N. A. N. Ouedraogo, Y. Chen, Y. Y. Xiao, Q. Meng, C. B. Han, H. Yan and Y. Zhang, "Stability of all-inorganic perovskite solar cells," Nano Energy, vol. 67, Jan. 2020, doi:10.1016/j.nanoen.2019.104249.

[8] J. Liang, C. Wang, Y. Wang, Z. Xu, Z. Lu, Y. Ma, H. Zhu, Y. Hu, C. Xiao, X. Yi, G. Zhu, H. Lv, L. Ma, T. Chen, Z. Tie, Z.Jin, J. Liu, "All-Inorganic Perovskite Solar Cells," Journal of the American Chemical Society, vol. 138, no. 49, Nov. 2016, doi: 10.1021/jacs.6b10227.

[9] P. Maji, S. Chatterjee, and S. Das, "Study on charge transportation and scaling behavior of CsPbI₃ microwires," Ceramics International, vol. 45, no. 5, Dec. 2019, doi: 10.1016/j.ceramint.2018.12.071.

[10] Q. Ma, S. Huang, X. Wen, M. A. Green and A. W. Y. Ho-Baillie, "Hole transport layer free inorganic $CsPbIBr_2$ perovskite solar cell by dual source thermal evaporation," Advanced energy materials, vol. 6, no. 7, Feb. 2016, doi:10.1002/aenm.201502202.

[11] C. Y. Chen, H. Y. Lin, K. M. Chiang, W. L. Tsai, Y. C. Huang, C. S. Tsao and H. W. Lin, "All vacuum deposited stoichiometrically balanced inorganic cesium lead halide perovskite solar cells with stabilized efficiency exceeding 11%," Advanced materials, vol. 29, no. 12, Jan. 2017, doi: 10.1002/adma.201605290.

[12] A. Kojima, K. Teshima, Y. Shirai, T. Miyasaka, "Organometal halide perovskites as visible-light sensitizers for photovoltaic cells," J. Am. Chem. Soc. vol. 131, no. 17, April. 2009, doi: 10.1021/ja809598r.

[13] Best-Research-Cell-Efficiencies.20190923.pdf, National Renewable Energy Laboratory, Research institute in Colorado, USA, 2019.

[14] L. G. Tejuca and J. L. G. Fierro, "Structure and Reactivity of Perovskite-Type Oxides," Advances in Catalysis, vol. 36, 1989, doi: 10.1016/S0360-0564(08)60019-X.

[15] Levy, Mark, "Crystal structure and defect properties in ceramic materials," Imperial College London thesis, Jan. 2005.

[16] G. S. Rohrer, "Structure and bonding in crystalline materials," Cambridge University Press, Feb. 2001, doi: 10.1017/CBO9780511816116.

[17] C. Li, X. Lu, W. Ding, L. Feng, Y. Gao and Z. Guo, "Formability of ABX_3 (X= F, Cl, Br, I) halide perovskites," Acta Crystallographica Section B: Structural Science, vol. 64, no. 6, Nov. 2008, doi: 10.1107/S0108768108032734.

[18] C. J. Bartel, C. Sutton, B. R. Goldsmith, R. Ouyang, C. B Musgrave, L. M. Ghiringhelli and M. Scheffler, "New tolerance factor to predict the stability of perovskite oxides and halides," Science advances, vol. 5, no. 2, Feb. 2019, doi: 10.1126/sciadv.aav0693.

[19] Hume-Rothery, W. Researches, "On the nature, properties, and conditions of formation of intermetallic compounds, with special reference to certain compounds of tin-I-V," Journal Institute of Metals, vol. 35, 1926.

[20] T. El Ashram, "Crystalline accommodation law explains the crystalline structure of materials," Journal of Advances in Physics, vol. 13, no. 8, 2017, doi: 10.24297/jap.v13i8.6295.

[21] International Center for Diffraction Data, PCPDFWIN v. 2.3, 1601 Park Lan, Swarthmore, PA 19081-2389, 2002 JCPDS, USA.

[22] K. Wang, Z. Jin, L. Liang, HuiBian, DongliangBai, H. Wang, J. Zhang, Q. Wang and S. Liu, "All-inorganic cesium lead iodide perovskite solar cells with stabilized efficiency beyond 15%," nature communications , vol. 9 , no. 4544, Oct. 2018, doi:10.1038/s41467-018-06915-6.

[23] A. Saparbaev, M. Zhang, V. Kuvondikov, L. Nurumbetova, I. O. Raji , I. Tajibaev, E. Zakhidov, X. Bao and R. Yang, "High-performance $CsPbI_3$ perovskite solar cells without additives in air condition," Solar Energy, vol. 228, Nov. 2021, doi: 10.1016/j.solener.2021.09.059.

[24] L. Duan, o. Zhang, M. Liu, M. Grätzel and J. Luo, "Phase-Pure γ-$CsPbI_3$ for Efficient Inorganic Perovskite Solar Cells," ACS Energy Letters, vol. 7, no. 9, Aug. 2022, doi: 10.1021/acsenergylett.2c01219.

[25] J. Wang, Y.Che, Y.Duan, Z. Liu, S. Yang, D. Xu, Z. Fang, X. Lei, Y. Li and S. F. Liu, "21.15%-Efficiency and Stable γ -$CsPbI_3$ Perovskite Solar Cells Enabled by an Acyloin Ligand," Advanced Materials, vol. 35, no. 12, Jan. 2023, doi: 10.1002/adma.202210223.